Cortical gyrification in relation to age and cognition in older adults

Sander Lamballais [a], Elisabeth J. Vinke [a,b], Meike W. Vernooij [a,b], M. Arfan Ikram [a], Ryan L. Muetzel [a,c,*]

[a] Department of Epidemiology, Erasmus MC University Medical Center Rotterdam, the Netherlands
[b] Department of Radiology and Nuclear Medicine, Erasmus MC University Medical Center Rotterdam, the Netherlands
[c] Department of Child and Adolescent Psychiatry, Erasmus MC University Medical Center Rotterdam, the Netherlands

ARTICLE INFO

ABSTRACT

Gyrification of the cerebral cortex changes with aging and relates to development of cognitive function during early life and midlife. Little is known about how gyrification relates to age and cognitive function later in life. We investigated this in 4397 individuals (mean age: 63.5 years, range: 45.7 to 97.9) from the Rotterdam Study, a population-based cohort. Global and local gyrification were assessed from T_1-weighted images. A measure for global cognition, the g-factor, was calculated from five cognitive tests. Older age was associated with lower gyrification (mean difference per year $= -0.0021$; 95% confidence interval $= -0.0025$; -0.0017). Non-linear terms did not improve the models. Age related to lower gyrification in the parietal, frontal, temporal and occipital regions, and higher gyrification in the medial prefrontal cortex. Higher levels of the g-factor were associated with higher global gyrification (mean difference per g-factor unit $= 0.0044$; 95% confidence interval $= 0.0015$; 0.0073). Age and the g-factor did not interact in relation to gyrification (p $>$ 0.05). The g-factor bilaterally associated with gyrification in three distinct clusters. The first cluster encompassed the superior temporal gyrus, the insular cortex and the postcentral gyrus, the second cluster the lingual gyrus and the precuneus, and the third cluster the orbitofrontal cortex. These clusters largely remained statistically significant after correction for cortical surface area. Overall, the results support the notion that gyrification varies with aging and cognition during and after midlife, and suggest that gyrification is a potential marker for age-related brain and cognitive decline beyond midlife.

1. Introduction

Gyrification is one of the most fundamental and distinguishing properties of the human cerebral cortex. The folding patterns of the cortex are highly heritable (Docherty et al., 2015), evolutionarily conserved, and similar amongst closely related animal species (Zilles et al., 2013). Abnormalities in gyrification, such as polymicrogyria and pachygyria, lead to altered brain function, which can manifest as impairments in speech and cognition. Similarly, both global and regional abnormalities in gyrification have been found in patients with autism (Duret et al., 2018; Blanken et al., 2015), schizophrenia (Matsuda and Ohi, 2018; Cao et al., 2017), and bipolar disorder (Cao et al., 2017). A deeper understanding of gyrification may therefore lead to better insight into a broad range of diseases.

Gyrification changes with age and in turn affects cognitive function (Cao et al., 2017; White et al., 2010; Gregory et al., 2016; Hogstrom et al.,

2013). The global degree of gyrification is often expressed as the Gyrification Index (GI). The GI peaks during childhood, rapidly declines during adolescence and the decline slows down as adulthood progresses (Cao et al., 2017; White et al., 2010; Gregory et al., 2016). Regional patterns of gyrification can be quantified with the Local Gyrification Index (LGI) (Schaer et al., 2008). The regions surrounding the angular gyrus, i.e. the parietal cortex, seem most prone to age-related decline in the LGI (Hogstrom et al., 2013). The association between the LGI and cognition has been studied in both pediatric and adult cohorts, and it showed the strongest effect in the frontal and parietal regions as well as the temporoparietal junction (Gregory et al., 2016). These findings consolidate the relevance of gyrification in the normal development of the brain.

Several knowledge gaps still remain. Limited work exists on cortical gyrification during middle adulthood, i.e. 40–65 years of age, and late adulthood, i.e. beyond 65 years of age. Other aspects of the cerebral

cortex – such as cortical surface area – change significantly during middle and late adulthood (Vinke et al., 2018). Furthermore, atrophy of the cerebral cortex seems to accelerates towards the end of life (Battaglini et al., 2019), and the rates of atrophy differ between brain regions (Vinke et al., 2018). How gyrification changes during late life and how the changes are distributed across the brain remains to be elucidated. Similarly, cognitive function declines in aging, which in turn may affect if and how cognition and gyrification relate. Finally, most previous studies were performed in clinical samples or clinic-based settings, limiting the external validity of the findings. The use of population-based studies would allow for better generalization of the results.

The aim of the present study was to elucidate the associations of age and cognition with gyrification during middle and late adulthood. The study was performed using data from the Rotterdam Study cohort, a prospective population-based cohort study of individuals aged 40 years and higher. We hypothesized that age and the GI showed a non-linear association across middle and late adulthood, where the rate of loss of gyrification accelerates with age. Furthermore, based on previous volumetric work, we expected to find that the shape of the association between age and the LGI differed across the brain, with regions near the angular gyrus showing the fastest decline towards the end of life. Finally, we hypothesized that cognition positively associated with the GI, and with the LGI in frontal and temporal regions.

2. Methods

2.1. Study population

The Rotterdam Study is a prospective cohort study based in the Ommoord district of Rotterdam, the Netherlands, that has been ongoing since 1989 (Ikram et al., 2017). The second recruitment wave started in 2000, and the third wave in 2006. All participants are re-invited for an interview and in-person examinations every 4–6 years. The study has included 14,926 participants 45 years of age and older. Neuroimaging was introduced in 2005 (Ikram et al., 2015). The current study population included individuals who were eligible to participate in a research center visit between 2006 and 2015 with cognitive testing and neuro-imaging (n = 6647). Of these, 38 had no cognitive test battery data, 980 had incomplete data, 417 did not participate in the MRI study, in 462 the image surface tesselation in FreeSurfer failed, and 145 were excluded due to poor quality of the T1-weighted images. We further excluded participants with prevalent stroke (n = 126) or prevalent dementia (n = 82). The final sample consisted of 4397 participants. A flow chart of the study population is shown in Supplementary Fig. 1. The Rotterdam Study has been approved by the Medical Ethics Committee of the Erasmus MC (registration number MEC 02.1015). All participants provided written informed consent.

2.2. Assessment of cognitive function

All participants underwent a cognitive test battery (Hoogendam et al., 2014). The battery consisted of five tests, each assessing different cognitive domains. The first test was the 15-word learning test (15WLT), to assess verbal learning and verbal memory (Bleecker et al., 1988). The 15WLT consisted of three trials where 15 words were presented visually, and after each trial participants had to name all words they could remember (i.e. immediate recall). At least 10 min after the third trial, participants were again asked to name all words that they could still remember (i.e. delayed recall). We used the number of words in the delayed condition as the measurement outcome. The second test was the Stroop task (Houx et al., 1993), a task that assesses selective attention and automaticity. Participants had to read aloud the names of colors (red, green, blue, yellow) as fast and flawless as possible. The words were printed on paper in mismatching colors (e.g. "blue" printed in the color red) to interfere with the naming process. The time to read all words was adjusted for the number of errors by calculating the time per word and

adding one-and-a-half that time for each error. Thus, the Stroop task is inversely coded compared to the other tests, where a higher score relates worse performance. The total was then log transformed and used as the outcome measure. The third test was the letter-digit substitution test (LDST) (van der Elst et al., 2006), in which participants have to write down the corresponding digits next to letters according to a dictionary table. This assesses processing speed as well as executive function. Fourth, a word fluency test (WFT) was administered to assess efficiency of searching long term memory (Welsh et al., 1994). Participants had to name as many animal species in a span of 1 min, with the total number of unique species as the outcome. Finally, we administered the Purdue pegboard test (PPB) (Tiffin and Asher, 1948), where participants had to place small metal pins into holes across three trials: left hand only, right hand only, and both hands. The sum of the number of pins over all trials was used as a measure for fine motor dexterity and psychomotor ability. To summarize all tests into a single score for global cognition, known as the g-factor, we used principal component analysis and isolated the first component (Deary, 2014). The g-factor explained 50.6% of the variance amongst the cognitive tests which is in agreement with previous literature (Deary, 2012).

2.3. Image acquisition

Neuroimaging was performed on a 1.5T magnetic resonance imaging (MRI) scanner with an eight-channel head coil (GE Signa Excite, General Electric Healthcare, Milwaukee, USA). The imaging sequences have been described extensively elsewhere (Ikram et al., 2015). Axial T_1-weighted images were collected using a 3D Spoiled Gradient Recalled sequence (T_R = 13.8 ms, T_E = 2.8 ms, T_I = 400 ms, flip angle = 20°, bandwidth = 12.5 kHz, voxel size = 0.8 mm isotropic). The images were subsequently stored in an extensible neuroimaging archive toolkit (XNAT) database (Marcus et al., 2007).

2.4. Image processing

Images were processed using the FreeSurfer analysis suite (version 6.0) (Fischl, 2012). The standard reconstruction was conducted, where non-brain tissue was removed, voxel intensities were corrected for B_1 field inhomogeneities, voxels were segmented into white matter, gray matter and cerebrospinal fluid, and surface-based models of gray and white matter were generated. The GI was calculated as the ratio between the outer contour of the cortex and the pial surface of the whole cerebrum. The LGI was estimated at each vertex along the cortical ribbon (Schaer et al., 2008, 2012), and each vertex was automatically assigned an anatomical label according to a predefined atlas (Desikan et al., 2006). All measures were co-registered to a standard stereotaxis space and smoothed with a full-width half-max Gaussian kernel, 5 mm for the LGI given inherent smoothness and 10 mm for all other measures.

A multistep procedure was used to identify datasets of insufficient quality for analysis. First, we used an automated tool to obtain a quality metric for each T_1-weighted scan that assesses artifacts related to motion (White et al., 2018). Next, we visually inspected FreeSurfer reconstructions from 200 randomly selected scans. The visual ratings consisted of inspecting segmented brain images in the coronal, sagittal and axial directions, as well as 3D reconstructions of the pial surface. The segmentation was rated as a fail if FreeSurfer did not succeed to consistently trace the white and pial surfaces. Next, we established that the automated quality metric value predicted strongly whether a test passed or failed. We subsequently set a threshold above which all scans were of sufficient quality, and all scans below the threshold were excluded.

2.5. Measurement of covariates

Hypertension was defined as a resting blood pressure exceeding 140/90 mmHg or the use of blood pressure lowering medication. Blood pressure was measured twice with a sphygmomanometer after 5 min of

rest, and the average of the two measurements was used. Use of blood pressure lowering medication was derived from information collected by a physician at the research center. Alcohol use was assessed during home interviews with questions based on beer, wine, liquor and other alcoholic beverages such as sherry and port. Based on these data, an established method was used to calculate alcohol in grams per day (Vliegenthart et al., 2002). BMI was calculating using the height and weight obtained during the research center visit. Smoking status was obtained during home interviews and individuals were classified as never smokers, past smokers or current smokers. Education level was assessed during the home visit interview and classified into four categories according to the United Nations Educational, Scientific and Cultural Organization classification: primary (no or primary education), low (unfinished secondary and lower vocational), intermediate (secondary or intermediate vocational) or high education (higher vocational or university).

2.6. Statistical analyses

All statistical analyses were performed in R 3.4.3 (R Core Team. R, 2016). To assess the relation of age and cognition with the GI we used linear regression models. Surface-based LGI analyses were performed to study the spatial distributions of these associations along the cortex. This was done with vertex-wise analyses using the R package QDECR (https://github.com/slamballais/QDECR). Resulting p-value maps were corrected for multiple comparisons at the vertex level using Gaussian Monte Carlo Simulations (Hagler et al., 2006). Surface-based analyses on cortical thickness and similar measures may show non-Gaussian patterns of spatial correlations, which would increase the false positive rate higher than 0.05[31]. We therefore set the cluster forming threshold to p = 0.001, as this has shown high correspondence with actual permutation testing across all surface measures (Greve and Fischl, 2018). We further applied Bonferroni correction to account for analyzing both hemispheres separately (i.e. p < 0.025 cluster-wise).

Age-related atrophy of the brain accelerates with age, which may also affect cortical gyrification. We therefore studied three types of associations between age and cortical gyrification: (1) a linear age term, (2) orthogonal linear and quadratic age terms, (3) a B-spline for age with two or three degrees of freedom. The spline knot for the two-fold spline was set at the median age, and the knots of the three-fold spline at the first and second tertiles. The shape of the relationship between age and gyrification was assessed in two steps by evaluating model fit. The linear and non-linear model fits for the GI were compared by calculating the Akaike information criterion (AIC) and the Bayesian information criterion (BIC) for each model. Next, we created a linear model for age and the LGI, and additionally a non-linear model depending on the AIC and BIC for the GI models.

Specific domains of cognition map to different functional regions of the cerebral cortex (Taylor et al., 2015). Therefore, in addition to the g-factor we also studied whether the scores from the individual cognitive tests associated with GI and LGI. Furthermore, to inspect whether the association between cognition and gyrification changes with age we created a separate model with an interaction term for age and the g-factor.

Models were adjusted for covariates to account for potential confounding. The age analyses were corrected for sex and for study cohort, i.e. the first, second or third cohort of the Rotterdam Study. The cognition analyses were adjusted in three separate models, which allows for the impact of each set of new confounders on model estimates to be described. Model 1 was adjusted for sex, cohort, age at cognitive testing and age difference between cognitive testing and the MRI scan. The way that age entered the model as a covariate – linear, quadratic or with splines – was dependent on the results from the analyses on age and the GI. Model 2 was additionally adjusted for hypertension, alcohol intake, smoking status and BMI. Lastly, Model 3 was additionally adjusted for education level. The p-values for the associations between the potential confounders and the global gyrification index are shown in

Supplementary Table 1. To assess whether image quality could affect the results we ran sensitivity analyses with the image quality metric for each scan as a covariate.

Gyrification is calculated as the ratio of the pial surface and the outer surface of the brain (Schaer et al., 2012). However, the cortical surface area itself has also been shown to relate to cognitive function (Cox et al., 2018). Any association between the LGI and cognition may therefore be driven by cortical surface area, and potentially by cortical thickness as well. To further assess this, we performed a sensitivity analysis per cluster. In each model we defined cognition as the outcome, and both the mean LGI and the mean cortical surface area or the mean cortical thickness of each cluster as the determinants. The models were further corrected for all covariates as used in Model 3. We then assessed whether the association between cognition and LGI remained statistically significant, taking into account cortical surface area or thickness.

All covariates had less than 1% missing data except for alcohol use (4.8%). In order to maximize power, missing covariate data were imputed thirty times using multiple imputation by chained equations (van Buuren and Groothuis-Oudshoorn, 2011). Imputed models were subsequently pooled per vertex according to Rubin's rules (Rubin, 1987). We also performed a non-response analysis to examine whether the individuals who were not included into the final sample were in any way different than those who were included (Table 1). This was done through logistic regression, where inclusion was entered as the outcome and all other variables were included as predictors.

Of note, in all models, we defined age or cognition as the determinants (predictors) and gyrification as the outcome, as limitations in vertex-wise analyses generally only allow for the vertex measure to be modeled as the outcome. Thus, while cognition is generally considered a consequence of brain structure, due to limitations in the vertex-wise software it was defined as a determinant of gyrification in the models. As a sensitivity analysis, we created models for each statistically

Table 1

Baseline characteristics of the study population. The excluded sample (n = 2250) were all participants that were eligible for cognitive testing and the neuroimaging study, but did not end up in the final sample (see Supplementary Fig. 1).

Characteristics	Included sample N = 4397	Excluded sample N = 2250	p-value[b]
Age at MRI (years)	63.5 ± 10.1	69.5 ± 1.13	<.001
G-factor	0.00 ± 1.00		
Cohort (%)			<.001
RS-I	15.3	33.9	
RS-II	25.3	26.7	
RS-III	59.4	39.5	
Sex, female (%)	55.3	57.8	.278
Time between cognition and MRI (years)	0.3 ± 0.4	0.2 ± 0.3	.847
Hypertensive (%)[a]	61.4	76.1	.053
Alcohol per day (grams)[a]	9.2 ± 10.1	8.5 ± 9.6	<.001
Body mass index (kg/m^2)[a]	27.4 ± 4.1	28.1 ± 4.8	.003
Smoking status (%)[a]			.406
Never	30.9	29.9	
Past	49.1	49.4	
Current	20.0	20.7	
Education level (%)[a]			.002
Primary	7.8	13.1	
Low	37.7	41.0	
Intermediate	30.3	28.4	
High	24.2	17.5	
Mean GI	2.55 ± 0.08	2.52 ± 0.09	<.001

MRI = Magnetic resonance imaging.

GI = Gyrification index.

[a] Missingness of data for all variables was below 1% except for alcohol consumption (4.8%).

[b] Differences between inclusion and exclusion were tested through multiple logistic regression.

significant LGI cluster where the cluster-wise mean LGI was defined as the determinant and the g-factor as the outcome.

All reported results focus on the beta coefficients and the 95% confidence intervals (CIs) rather than p-values. Confidence intervals give insight into the range of values within which the true parameter will likely be, whereas p-values do not (Greenland et al., 2016). Any reported result that is stated as statistically significant will have a p-value below the threshold of 0.05.

3. Results

Baseline characteristics of the study population (n = 4397) are displayed in Table 1. The mean age of the participants was 63.5 years (SD: 10.1, range: 45.7 to 97.9) and 55.3% were female. We analyzed whether any differences were present between individuals included in the

analysis and those who were eligible for MRI but did not end up in the final sample (Supplementary Fig. 1). Excluded participants tended to be older (mean = 6.2 years), were more often from the first cohort of the Rotterdam Study (33.9% versus 15.3%), were less likely to drink alcohol (mean = −0.7 g per day), had a higher BMI (mean = 0.7 kg/m^2), were more likely to have only primary education (13.1% versus 7.8%) and had a lower GI (mean = −0.03).

3.1. Age and global gyrification

A scatterplot of age and the GI is shown in Fig. 1A, and the results of the different models are shown in Table 2. In the linear model one year increase in age associated with a −0.0021 (95% CI: -0.0025; −0.0017) lower GI. For the 2nd polynomial model both the linear term (p < 0.001) and the quadratic term (p = 0.027) were also statistically significant. All
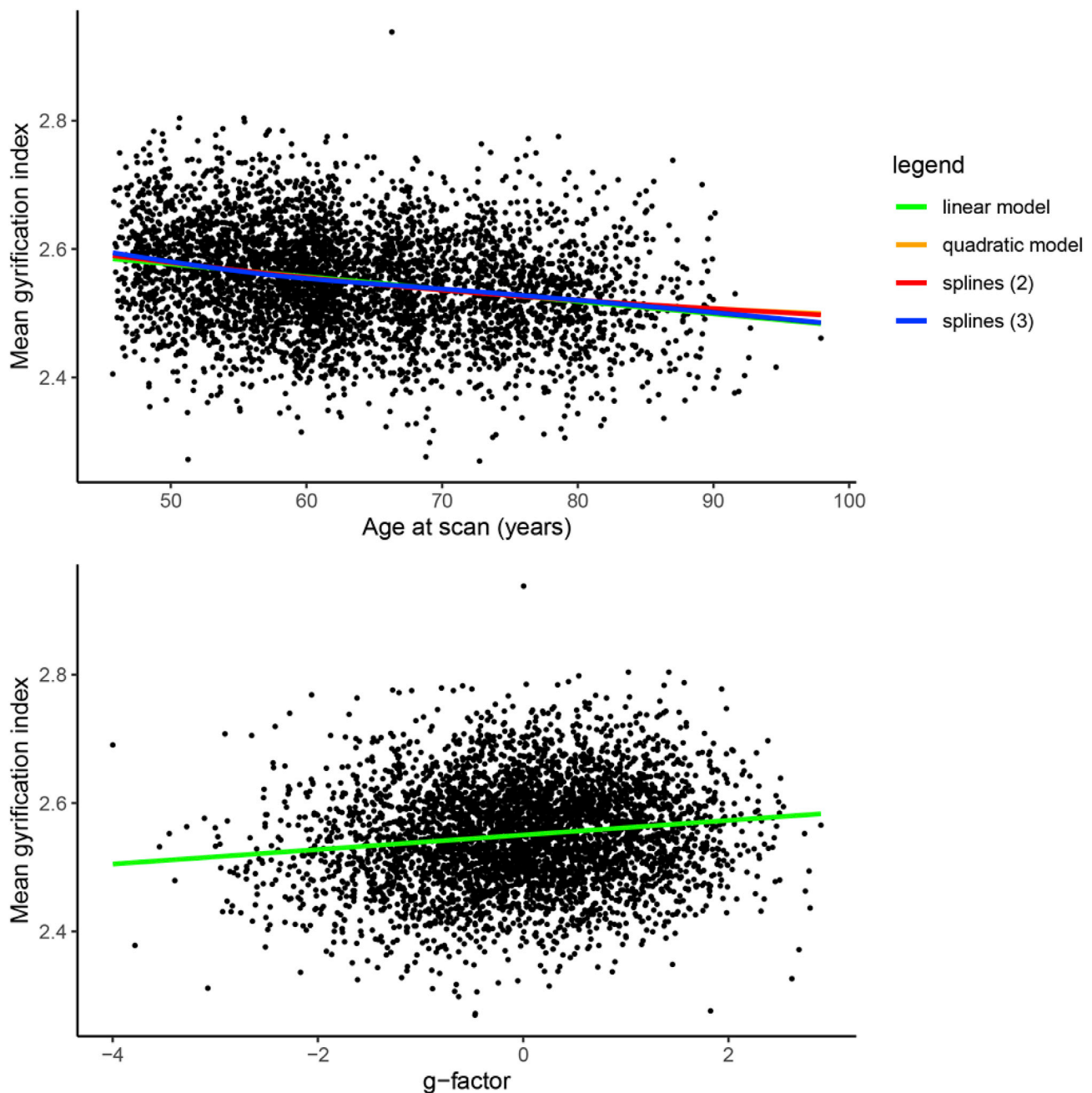

Fig. 1. Scatterplot of age (A) and cognition (B) with GI. For age, four models were plotted (linear, quadratic, and the two and three spline models). The lines are not fully visible due to the extensive overlap. The plot for cognition only shows the linear model.

Table 2
The associations between age and GI.

Model[a]	Type	β	95% CI	AIC	BIC
Linear	Linear	−0.0021	−0.0025; −0.0017	−10252.60	−10214.27
Quadratic	1st polynomial	−0.0053	−0.0081; −0.0024	−10255.47	−10210.75
	2nd polynomial	−0.000025	−0.000003; −0.000046		
Spline (2)	1st spline	−0.1235	−0.2376; −0.1020	−10256.33	−10211.61
	2nd spline	−0.0703	−0.0947; −0.0458		
Spline (3)	1st spline	−0.0552	−0.0384; −0.0718	−10203.46	−10254.57
	2nd spline	−0.1179	−0.0915; −0.1442		
	3rd spline	−0.0826	−0.0550; −0.1102		

GI = Gyrification index.
CI = Confidence interval.
AIC = Akaike information criterion.
BIC = Bayesian information criterion.
[a] The models were adjusted for study cohort and sex.

spline coefficients were statistically significant for the natural cubic splines with both two and three degrees of freedom. The AIC and BIC of all models were highly similar, suggesting that the linear fit sufficiently describes the association of age during mid and late adulthood with the GI.

3.2. Cognition and global gyrification

A scatterplot of the g-factor and the GI is shown in Fig. 1B, and regression coefficients for the g-factor and all separate cognitive tests are shown in Table 3 for all three adjustment models. Higher levels of the g-factor were associated with a higher GI, with similar results across Model 1 (β = 0.0045, 95% CI = 0.0018; 0.0073) to Model 3 (β = 0.0044, 95% CI = 0.0015; 0.0073). We examined the individual cognitive tests to see which cognitive tests drove most of the association. Three cognitive tests yielded statistically significant results, namely the LDST (β = 0.0005, 95% CI = 0.0001; 0.0009), the WFT (β = 0.0009, 95% CI = 0.0005; 0.0013) and the Stroop task (β = −0.0081, 95% CI = −0.0164; −0.0002). Of these, the Stroop task had the strongest association with gyrification. Of note is that the association with the Stroop task was negative due to the lower scores on the Stroop task reflecting higher cognitive performance. Finally, the interaction term between age and cognition did not reach statistical significance in any of the models (all $p_{unadjusted} > 0.05$), thus the magnitude of the association between cognition and the GI was stable during and after midlife.

3.3. Age and local gyrification

In order to determine the precise spatial extent of associations between age and gyrification, we performed surface-based vertex-wise

analyses. Due to the similar fits between the models of age and the GI we opted to further investigate the linear model and the two-fold spline model with the LGI. Fig. 2 displays the vertex-wise associations between age and the LGI. In the linear model the LGI decreased with age in the parietal, temporal, occipital and frontal regions. The effect sizes were generally larger than those found when examining the association between age and the GI. A second cluster arose in the frontal pole and medial prefrontal cortex, where the LGI increased with age. The significant clusters were similar across hemispheres in both size and strength. The two-degree spline model differed from the linear model. The first spline fold, i.e. ages between 45.7 and 61.6 years, associated negatively with the LGI in the parietal, frontal, temporal and occipital regions. Unlike the linear model, no cluster was present near the frontal pole or the medial prefrontal pole. In the second spline fold, i.e. ages between 61.6 and 97.9 years, the negative associations were more restricted to the temporal and parietal regions, and the lateral part of the frontal cortex. In addition, a positive cluster was present in the medial prefrontal cortex and the frontal pole, stronger than in the linear model. The age-gyrification association shows a clear deviation in its shape in the medial prefrontal gyrus compared to other regions (Supplementary Fig. 2). The findings were robust upon further correction for the image quality metric (Supplementary Fig. 3).

3.4. Cognition and local gyrification

Fig. 3 displays the vertex-wise associations of the g-factor with the LGI for the three adjustment models. Associations between g-factor and the LGI were mostly present in three clusters: (1) the superior temporal gyrus, the insular cortex and the postcentral gyrus, (2) the lingual gyrus, the precuneus and the pericalcarine cortex and (3) the orbitofrontal

Table 3
The associations between cognition and the GI.

Domain	GI (Model 1[a])		GI (Model 2[b])		GI (Model 3[c])	
	β	95% CI	β	95% CI	β	95% CI
g-factor	0.0045	0.0018; 0.0073	0.0047	0.0019; 0.0075	0.0044	0.0015; 0.0073
15WLT	−0.0001	−0.0009; 0.0007	−0.0001	−0.0010; 0.0007	−0.0003	−0.0011; 0.0006
Stroop task[d]	−0.0090	−0.0171; −0.0010	−0.0090	−0.0172; −0.0010	−0.0081	−0.0164; −0.0002
LDST	0.0005	0.0001; 0.0009	0.0005	0.0002; 0.0009	0.0005	0.0001; 0.0009
WFT	0.0009	0.0005; 0.0013	0.0009	0.0005; 0.0013	0.0009	0.0005; 0.0013
PPB	0.0001	−0.0004; 0.0007	0.0002	−0.0004; 0.0007	0.0002	−0.0004; 0.0007

WLT = 15 Word learning test.
LDST = Letter digit substitution test.
WFT = Word fluency test.
PPB = Purdue pegboard test.
CI = Confidence interval.
[a] Adjusted for age at MRI scan (years), study cohort, sex and age difference between cognitive testing and MRI scan (years).
[b] Additionally adjusted for hypertension (yes/no), alcohol intake (grams per day), BMI and smoking status (never/past/current).
[c] Additionally adjusted for education level (primary/low/intermediate/high).
[d] The Stroop task is inversely coded compared to the other tests, where a higher score relates worse performance.
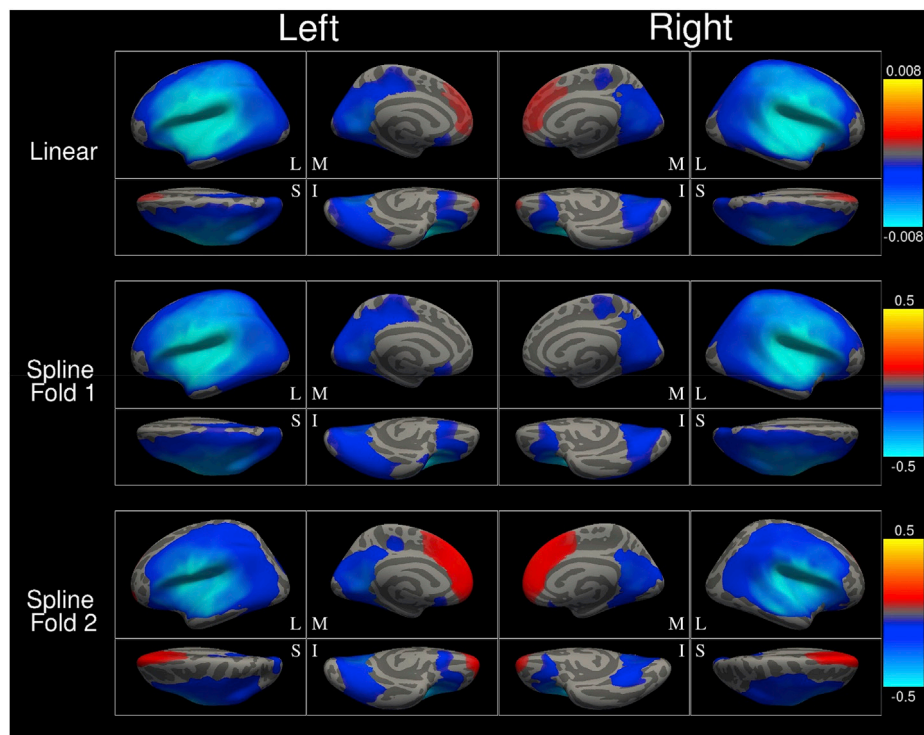
Fig. 2. Vertex-wise associations between age – the linear model and the two-fold spline model – and the local gyrification index (LGI). The color scale represents the regression coefficients. The models were adjusted for study cohort and sex. L = Lateral; M = Medial; S = Superior; I = Inferior.
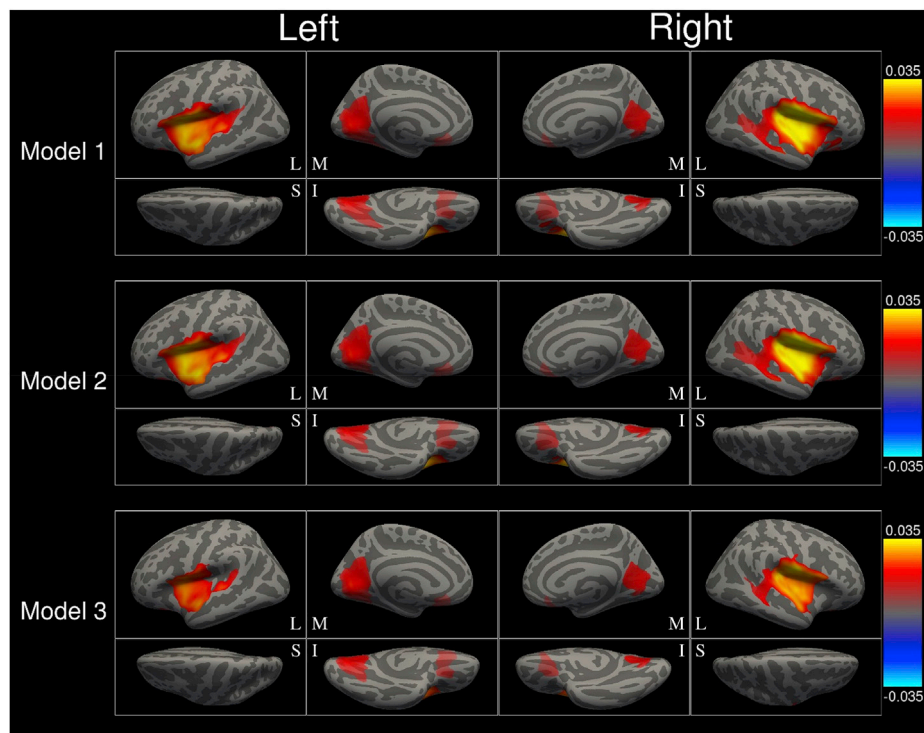

Fig. 3. Vertex-wise associations between the g-factor and the LGI. The color scale represents the regression coefficients. Model 1 was adjusted for age (linear term), study cohort, sex and the time difference between the cognitive test battery and the MRI visit. Model 2 was additionally adjusted for hypertension status, alcohol intake, BMI and smoking. Model 3 was additionally adjusted for education level. L = Lateral; M = Medial; S = Superior; I = Inferior.

gyrus. These clusters roughly presented bilaterally. Similar patterns were found for the associations between the individual cognitive tests and the LGI (Fig. 4). The LGI of the cuneate gyrus, insular cortex and superior temporal gyrus were all associated with the Stroop task, the LDST and the

WFT, although more so on the right than the left hemisphere. Additionally, the WFT also associated with the LGI in several additional regions, namely the supramarginal gyrus on both hemispheres and the lateral orbitofrontal cortex, the angular gyrus and the superior parietal
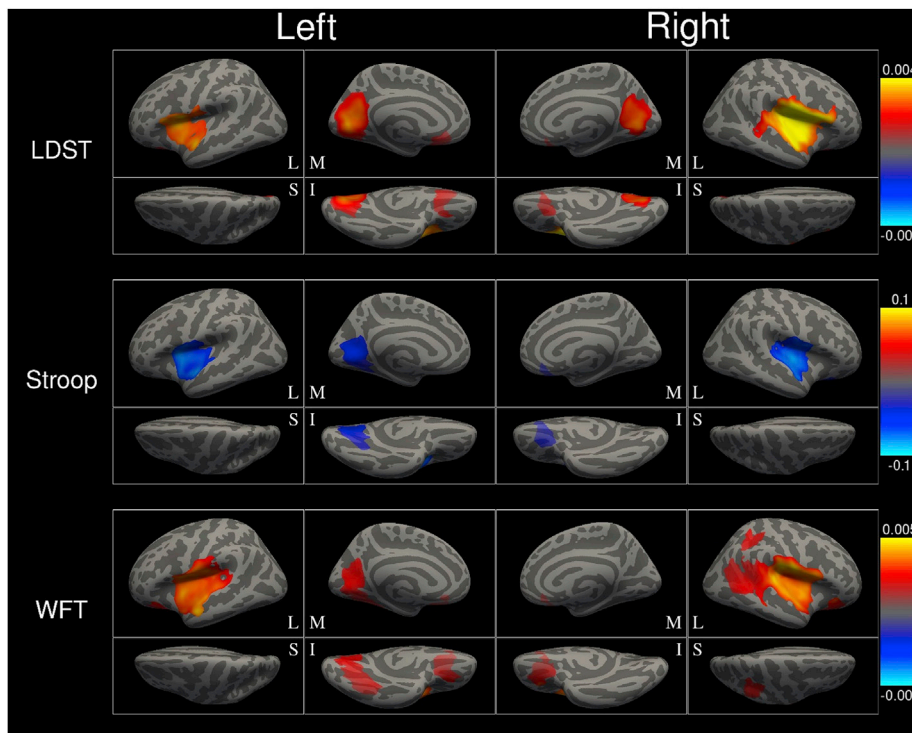
Fig. 4. Associations between the individual cognitive tests and the LGI. The color scale represents the regression coefficients. The images show the results for Adjustment Model 3. The Stroop task is inversely coded compared to the other tests, where a higher score relates worse performance. No statistically significant clusters were identified for the 15 word learning test or the Purdue pegboard test, thus these are not displayed. LDST = Letter digit substitution test; WFT = Word fluency test. L = Lateral; M = Medial; S = Superior; I = Inferior.

gyrus on the right hemisphere. Further correction for the image quality metric did not affect these findings (Supplementary Fig. 4). Finally, as cognition was originally specified as the determinant, we constructed cluster-wise models with the cluster-wise mean gyrification as the determinant and cognition as the outcome. For the identified LGI clusters the associations with cognition remained unattenuated (all clusters p < 0.00001).

Both vertex-wise cortical surface area and thickness associate with age (Supplementary Fig. 5) and the g-factor (Supplementary Fig. 6). In order to assess whether the associations between cognition and the LGI were driven by cortical surface area or thickness, we created a new model for each significant LGI cluster with the g-factor as the outcome and both the mean LGI and the mean cortical thickness or surface area as determinants. Associations remaining after concurrent adjustment for cortical surface area or thickness suggest an independence between LGI the other measures. The results are shown in Table 4 for surface area and in Table 5 for cortical thickness. After adjustment for surface area, the LGI remained associated with the g-factor in the left hemisphere in the cluster near the cuneus ($p_{unadjusted}$ = .002) but not the clusters in the orbitofrontal cortex ($p_{unadjusted}$ = .056) or the temporal cortex ($p_{unadjusted}$ = .115). In the right hemisphere the association between the LGI and cognition was unaffected by surface area in both the orbitofrontal ($p_{unadjusted}$ = .019) and the temporal clusters ($p_{unadjusted}$ = .004), but not in the cluster in the cuneus ($p_{unadjusted}$ = .094). In all clusters, the LGI was unaffected by additional corrections for cortical thickness.

4. Discussion

We show in a large population-based setting that global gyrification of the cerebral cortex decreases during middle and late adulthood. This decline in gyrification is mainly driven by regions close to the Sylvian fissure. A specific cluster within the medial prefrontal cortex showed more gyrification with increasing age, particularly during late adulthood. Furthermore, we also found that global cognition positively associates with gyrification, in particular in the temporal regions, the lingual gyrus and the cuneus.

The findings for age and gyrification are in line with previously

reported findings in smaller or younger age samples. A study from 2017 attempted to map the life course trajectory of the GI in a cross-sectional sample of 881 participants (Cao et al., 2017). The authors found that the GI trajectory can be described as a negative logarithmic function, with the decline in gyrification slowing with age. However, their sample included only about 30 participants above the age of 60. Another study reported on the association of age and gyrification in 322 healthy adults of whom 116 were aged 60 or older (Hogstrom et al., 2013). They found that the LGI had non-linear associations with age in certain brain regions, especially the orbitofrontal and dorsomedial prefrontal cortex. In particular, LGI in these regions seemed to increase towards the end of life. Our study builds upon these findings, with a much larger number of participants beyond the age of 70 years, allowing us to more precisely study how gyrification changes during late adulthood. We found that the association is essentially linear, which matches a negative logarithmic life course pattern (Cao et al., 2017). We also established non-linear patterns in the regional surface-based patterns, albeit the increase in LGI was only seen in the medial prefrontal cortex and only towards the end of life. These findings further consolidate the global and local dependence of gyrification on age.

Gyrification associates with cognition during and after midlife, and this association does not change with age. Furthermore, in half of the significant clusters we found that cortical surface area is likely driving the associations. This is not surprising as loss of surface area leads to lower folding thus lower gyrification within that region. Still, three out of six LGI clusters remained associated with cognition after adjusting for surface area, suggesting that gyrification harbors independent information. Furthermore, the pattern of LGI clusters within our study was similar amongst the individual cognitive tests, suggesting that the LGI captures a more general aspect of cognitive function. Gyrification may therefore play a unique role in cognitive function, which could prove useful in the study of normal and abnormal cognitive aging. For example, other cortical characteristics such as thickness and surface area have distinct contributions to cognitive decline as seen in Alzheimer's disease (Yang et al., 2019; Ossenkoppele et al., 2019; Dickerson et al., 2009), yet any such contributions from gyrification remain to be elucidated.

The temporal lobe has previously been linked to cognitive processes

Table 4

The associations of the mean LGI and mean surface area with g-factor per previously identified LGI cluster. Each model contained both LGI and surface area. Both the LGI and surface area were standardized in order to be able to compare the magnitude of their effects. All models were adjusted for age at MRI scan (years), study cohort, sex, age difference between cognitive testing and MRI scan (years), hypertension (yes/no), alcohol intake (grams per day), BMI (kg/m^2), smoking status (never/past/current), and education level (primary/low/intermediate/high).

Hemisphere	#	Location	Standardized mean LGI			standardized mean surface area		
			β	95% CI	p	β	95% CI	p
Left	1	Temporal	0.025	[-0.006; 0.055]	.115	0.056	[0.024; 0.088]	.001
Left	2	Cuneus	0.047	[0.016; 0.077]	.002	0.025	[-0.005; 0.056]	.106
Left	3	Orbitofrontal	0.025	[-0.001; 0.050]	.056	0.067	[0.038; 0.096]	<.001
Right	1	Temporal	0.045	[0.014; 0.076]	.004	0.041	[0.009; 0.073]	.012
Right	2	Cuneus	0.028	[-0.005; 0.073]	.094	0.029	[-0.004; 0.063]	.085
Right	3	Orbitofrontal	0.030	[0.005; 0.054]	.019	0.061	[0.034; 0.089]	<.001

Table 5

The associations of the mean LGI and mean cortical thickness with g-factor per previously identified LGI cluster. Each model contained both LGI and cortical thickness. Both the LGI and cortical thickness were standardized in order to be able to compare the magnitude of their effects. All models were adjusted for age at MRI scan (years), study cohort, sex, age difference between cognitive testing and MRI scan (years), hypertension (yes/no), alcohol intake (grams per day), BMI (kg/m^2), smoking status (never/past/current), and education level (primary/low/intermediate/high).

Hemisphere	#	Location	Standardized mean LGI			standardized mean thickness		
			β	95% CI	p	β	95% CI	p
Left	1	Temporal	0.063	[0.038; 0.088]	<.001	0.062	[0.039; 0.085]	<.001
Left	2	Cuneus	0.069	[0.045; 0.094]	<.001	0.045	[0.022; 0.068]	<.001
Left	3	Orbitofrontal	0.044	[0.020; 0.068]	<.001	−0.025	[-0.049; −0.000]	.047
Right	1	Temporal	0.075	[0.050; 0.100]	<.001	0.061	[0.037; 0.085]	<.001
Right	2	Cuneus	0.058	[0.034; 0.083]	<.001	0.050	[0.027; 0.073]	<.001
Right	3	Orbitofrontal	0.049	[0.026; 0.073]	<.001	−0.003	[-0.027; 0.021]	.790

such as language (Price, 2012) and memory (Jeneson and Squire, 2012) as well as psychiatric disorders like adulthood autism spectrum disorders (Kohli et al., 2019) and schizophrenia (Palaniyappan and Liddle, 2012; Nesvag et al., 2014; Madre et al., 2019). Interestingly, these disorders have also been linked to abnormal gyrification (Duret et al., 2018; Blanken et al., 2015; Matsuda and Ohi, 2018; Cao et al., 2017). Genetic mechanisms underlying cognitive processes and neuropsychiatric disorders may also affect cortical morphology in the temporal region, and in particular gyrification. Previous studies have found links between genes underlying cognition function and temporal lobe structure (Tan et al., 2019; Ersland et al., 2012), although the results are inconsistent (van der Lee et al., 2019). Thus further work is needed to elucidate the presence of a genetic pleiotropic link between gyrification and function of the temporal lobe.

Several mechanisms could explain how gyrification changes with age. One explanation is that during brain development the cortical surface buckles due to differential rates of growth of cortical layers (Richman et al., 1975), and the opposite may occur during adulthood. The rate of atrophy is higher in gray than white matter during early and mid adulthood (Taki et al., 2011; Schippling et al., 2017). Gray matter atrophy is mostly through the reduction of surface area of the cortex, which leads to more shallow sulci and consequently a lower GI. The rate of atrophy of white matter starts to exceed the rate for gray matter during late adulthood (Vinke et al., 2018), which could in turn lead to an increase in gyrification with age. Interestingly, a previous study found that after the age of 60 years the cingulate cortex thickens and that the rate of thinning of the medial prefrontal cortex declines (Fjell et al., 2014), which could explain the increased gyrification of the medial prefrontal cortex in our study. Indeed, we see a similar thinning of the cingulate cortex. However, our findings also suggest that gyrification overall keeps decreasing during older adulthood, thus other mechanisms than the different gray and white matter atrophy rates are also likely involved.

Another plausible explanation is the "axon tension" theory (Van Essen, 1997), which states that axonal tension pulls the gyral walls inwards, thus folding the cortex. The axonal tension may depend on the health status of the axon, and damage to axons could lead to reduced tension and consequently decreased gyrification. White matter

microstructure decreases with age (Inano et al., 2011; Burzynska et al., 2017) and white matter lesions accumulate from mid adulthood onwards (Vinke et al., 2018), and could explain the decrease in gyrification. However, further experimental work has discredited axonal tension as a cause of cortical folding. For example, if axonal tension causes gyrification then cutting the gyrus transaxially should unfold the gyrus, and experiments have shown that this is not the case (Xu et al., 2010). Thus, further work is needed to elucidate the causes of cortical (un)folding during adulthood.

Gyrification may also associate with age due to more technical aspects of the data collection itself. Head motion may affect the relation between age and GI (Madan and Kensinger, 2017). The reasoning for this is that older participants tend to move more with their head while in the MRI. A previous study confirmed this and also found that head motion related to LGI, although the association was not very strong (Madan, 2018). We attempted to minimize the impact of head motion on the analyses by conservatively excluding all raw images with suboptimal quality and further by performing sensitivity analyses with the image quality metric as a covariate.

The study has several limitations. First of all, we relied on a cross-sectional study design to examine age effects on gyrification. Cross-sectional estimation of age-related changes may yield inaccurate estimates compared to longitudinal designs (Pfefferbaum and Sullivan, 2015). Second, changes in gyrification likely cause changes in cognition, but the models were specified with cognition as the determinant and gyrification as the outcome due to limitations in the vertex-wise analysis modeling. Rerunning the models per cluster with proper specification did show that the LGI clusters indeed associated with cognition, suggesting that the models hold under proper specification. Third, the cognitive test battery that was used does not cover all aspects of cognitive function. Due to the emphasis on verbal tests we were not able to fully assess the scope of cognition and gyrification. Fourth, in the case of cognition there may be reverse causality, as higher intelligence tends to lead to a healthier lifestyle and thus better brain health. We corrected for a number of variables related to lifestyle and their effect on the association was minimal. Despite this there could still be residual confounding by other variables that we did not account for. Fifth, while we excluded those with

prevalent stroke and dementia, there could be other medical conditions and confounders that could bias the results. For example, traumatic brain injury and substance abuse disorders are known to accelerate brain and cognitive aging (Wood, 2017; Cole et al., 2015; Mende, 2019), and could subsequently affect the association of age and cognition with gyrification. Our study also had several strengths. First, this is the largest sample size to date in a study of gyrification and age or cognition, leading to sufficient statistical power to find associations, and unravel new regional differences. Second, the individuals were sampled from a wide age-range, thus enabling making accurate inferences about gyrification even in the later phases of late adulthood. Third, the sample was drawn from a population-based cohort, thus the findings can be generalized beyond a clinical setting.

In conclusion, gyrification globally decreases linearly with age across the entirety of adulthood, and gyrification in the medial prefrontal cortex increases towards the end of life. Furthermore, gyrification increases with higher levels of cognitive performance in some clusters irrespective of surface area. These findings consolidate the importance of gyrification in normal brain function. Whether gyrification is a viable marker for abnormal brain aging and cognitive decline towards the end of life remains to be elucidated.

Disclosures

Declaration of competing interest

The authors report no potential conflicts of interest.

CRediT authorship contribution statement

Sander Lamballais: Conceptualization, Software, Formal analysis, Writing - original draft, Visualization. **Elisabeth J. Vinke:** Conceptualization, Formal analysis, Writing - review & editing. **Meike W. Vernooij:** Resources, Writing - review & editing. **M. Arfan Ikram:** Conceptualization, Resources, Funding acquisition, Writing - review & editing. **Ryan L. Muetzel:** Conceptualization, Writing - original draft, Supervision.

Acknowledgements

Appendix A. Supplementary data

Supplementary data to this article can be found online at https://doi.org/10.1016/j.neuroimage.2020.116637.

References

Battaglini, M., Gentile, G., Luchetti, L., Giorgio, A., Vrenken, H., Barkhof, F., Cover, K.S., Bakshi, R., Chu, R., Sormani, M.P., Enzinger, C., Ropele, S., Ciccarelli, O., Wheeler-Kingshott, C., Yiannakas, M., Filippi, M., Rocca, M.A., Preziosa, P., Gallo, A., Bisecco, A., Palace, J., Kong, Y., Horakova, D., Vaneckova, M., Gasperini, C., Ruggieri, S., De Stefano, N., Group, M.S., 2019. Lifespan normative data on rates of brain volume changes. Neurobiol. Aging 81, 30–37.

Blanken, L.M., Mous, S.E., Ghassabian, A., Muetzel, R.L., Schoemaker, N.K., El Marroun, H., van der Lugt, A., Jaddoe, V.W., Hofman, A., Verhulst, F.C., Tiemeier, H., White, T., 2015. Cortical morphology in 6- to 10-year old children with autistic traits: a population-based neuroimaging study. Am. J. Psychiatr. 172, 479–486.

Bleecker, M.L., Bolla-Wilson, K., Agnew, J., Meyers, D.A., 1988. Age-related sex differences in verbal memory. J. Clin. Psychol. 44, 403–411.

Burzynska, A.Z., Jiao, Y., Knecht, A.M., Fanning, J., Awick, E.A., Chen, T., Gothe, N., Voss, M.W., McAuley, E., Kramer, A.F., 2017. White matter integrity declined over 6-months, but dance intervention improved integrity of the fornix of older adults. Front. Aging Neurosci. 9, 59.

van Buuren, S., Groothuis-Oudshoorn, K., 2011. Mice: multivariate imputation by chained equations in r. J. Stat. Software 45, 1–67.

Cao, B., Mwangi, B., Passos, I.C., Wu, M.J., Keser, Z., Zunta-Soares, G.B., Xu, D., Hasan, K.M., Soares, J.C., 2017. Lifespan gyrification trajectories of human brain in healthy individuals and patients with major psychiatric disorders. Sci. Rep. 7, 511.

Cole, J.H., Leech, R., Sharp, D.J., 2015. Alzheimer's Disease Neuroimaging I. Prediction of brain age suggests accelerated atrophy after traumatic brain injury. Ann. Neurol. 77, 571–581.

Cox, S.R., Bastin, M.E., Ritchie, S.J., Dickie, D.A., Liewald, D.C., Munoz Maniega, S., Redmond, P., Royle, N.A., Pattie, A., Valdes Hernandez, M., Corley, J., Aribisala, B.S., McIntosh, A.M., Wardlaw, J.M., Deary, I.J., 2018. Brain cortical characteristics of lifetime cognitive ageing. Brain Struct. Funct. 223, 509–518.

Deary, I.J., 2012. Intelligence. Annu. Rev. Psychol. 63, 453–482.

Deary, I.J., 2014. The stability of intelligence from childhood to old age. Curr. Dir. Psychol. Sci. 23.

Desikan, R.S., Segonne, F., Fischl, B., Quinn, B.T., Dickerson, B.C., Blacker, D., Buckner, R.L., Dale, A.M., Maguire, R.P., Hyman, B.T., Albert, M.S., Killiany, R.J., 2006. An automated labeling system for subdividing the human cerebral cortex on mri scans into gyral based regions of interest. Neuroimage 31, 968–980.

Dickerson, B.C., Feczko, E., Augustinack, J.C., Pacheco, J., Morris, J.C., Fischl, B., Buckner, R.L., 2009. Differential effects of aging and alzheimer's disease on medial temporal lobe cortical thickness and surface area. Neurobiol. Aging 30, 432–440.

Docherty, A.R., Hagler Jr., D.J., Panizzon, M.S., Neale, M.C., Eyler, L.T., Fennema-Notestine, C., Franz, C.E., Jak, A., Lyons, M.J., Rinker, D.A., Thompson, W.K., Tsuang, M.T., Dale, A.M., Kremen, W.S., 2015. Does degree of gyrification underlie the phenotypic and genetic associations between cortical surface area and cognitive ability? Neuroimage 106, 154–160.

Duret, P., Samson, F., Pinsard, B., Barbeau, E.B., Bore, A., Soulieres, I., Mottron, L., 2018. Gyrification changes are related to cognitive strengths in autism. Neuroimage Clin. 20, 415–423.

van der Elst, W., van Boxtel, M.P., van Breukelen, G.J., Jolles, J., 2006. The letter digit substitution test: normative data for 1,858 healthy participants aged 24-81 from the maastricht aging study (maas): influence of age, education, and sex. J. Clin. Exp. Neuropsychol. 28, 998–1009.

Ersland, K.M., Christoforou, A., Stansberg, C., Espeseth, T., Mattheisen, M., Mattingsdal, M., Hardarson, G.A., Hansen, T., Fernandes, C.P., Giddaluru, S., Breuer, R., Strohmaier, J., Djurovic, S., Nothen, M.M., Rietschel, M., Lundervold, A.J., Werge, T., Cichon, S., Andreassen, O.A., Reinvang, I., Steen, V.M., Le Hellard, S., 2012. Gene-based analysis of regionally enriched cortical genes in gwas data sets of cognitive traits and psychiatric disorders. PloS One 7, e31687.

Van Essen, D.C., 1997. A tension-based theory of morphogenesis and compact wiring in the central nervous system. Nature 385, 313–318.

Fischl, B., 2012. Freesurfer. Neuroimage 62, 774–781.

Fjell, A.M., Westlye, L.T., Grydeland, H., Amlien, I., Espeseth, T., Reinvang, I., Raz, N., Dale, A.M., Walhovd, K.B., 2014. Alzheimer Disease Neuroimaging I. Accelerating cortical thinning: unique to dementia or universal in aging? Cerebr. Cortex 24, 919–934.

Greenland, S., Senn, S.J., Rothman, K.J., Carlin, J.B., Poole, C., Goodman, S.N., Altman, D.G., 2016. Statistical tests, p values, confidence intervals, and power: a guide to misinterpretations. Eur. J. Epidemiol. 31, 337–350.

Gregory, M.D., Kippenhan, J.S., Dickinson, D., Carrasco, J., Mattay, V.S., Weinberger, D.R., Berman, K.F., 2016. Regional variations in brain gyrification are associated with general cognitive ability in humans. Curr. Biol. 26, 1301–1305.

Greve, D.N., Fischl, B., 2018. False positive rates in surface-based anatomical analysis. Neuroimage 171, 6–14.

Hagler Jr., D.J., Saygin, A.P., Sereno, M.I., 2006. Smoothing and cluster thresholding for cortical surface-based group analysis of fmri data. Neuroimage 33, 1093–1103.

Hogstrom, L.J., Westlye, L.T., Walhovd, K.B., Fjell, A.M., 2013. The structure of the cerebral cortex across adult life: age-related patterns of surface area, thickness, and gyrification. Cerebr. Cortex 23, 2521–2530.

Hoogendam, Y.Y., Hofman, A., van der Geest, J.N., van der Lugt, A., Ikram, M.A., 2014. Patterns of cognitive function in aging: the rotterdam study. Eur. J. Epidemiol. 29, 133–140.

Houx, P.J., Jolles, J., Vreeling, F.W., 1993. Stroop interference: aging effects assessed with the stroop color-word test. Exp. Aging Res. 19, 209–224.

Ikram, M.A., van der Lugt, A., Niessen, W.J., Koudstaal, P.J., Krestin, G.P., Hofman, A., Bos, D., Vernooij, M.W., 2015. The rotterdam scan study: design update 2016 and main findings. Eur. J. Epidemiol. 30, 1299–1315.

Ikram, M.A., Brusselle, G.G.O., Murad, S.D., van Duijn, C.M., Franco, O.H., Goedegebure, A., Klaver, C.C.W., Nijsten, T.E.C., Peeters, R.P., Stricker, B.H., Tiemeier, H., Uitterlinden, A.G., Vernooij, M.W., Hofman, A., 2017. The rotterdam

study: 2018 update on objectives, design and main results. Eur. J. Epidemiol. 32, 807–850.

Inano, S., Takao, H., Hayashi, N., Abe, O., Ohtomo, K., 2011. Effects of age and gender on white matter integrity. AJNR Am. J. Neuroradiol. 32, 2103–2109.

Jeneson, A., Squire, L.R., 2012. Working memory, long-term memory, and medial temporal lobe function. Learn. Mem. 19, 15–25.

Kohli, J.S., Kinnear, M.K., Martindale, I.A., Carper, R.A., Muller, R.A., 2019. Regionally decreased gyrification in middle-aged adults with autism spectrum disorders. Neurology 93, e1900–e1905.

van der Lee, S.J., Knol, M.J., Chauhan, G., Satizabal, C.L., Smith, A.V., Hofer, E., Bis, J.C., Hibar, D.P., Hilal, S., van den Akker, E.B., Arfanakis, K., Bernard, M., Yanek, L.R., Amin, N., Crivello, F., Cheung, J.W., Harris, T.B., Saba, Y., Lopez, O.L., Li, S., van der Grond, J., Yu, L., Paus, T., Roshchupkin, G.V., Amouyel, P., Jahanshad, N., Taylor, K.D., Yang, Q., Mathias, R.A., Boehringer, S., Mazoyer, B., Rice, K., Cheng, C.Y., Maillard, P., van Heemst, D., Wong, T.Y., Niessen, W.J., Beiser, A.S., Beekman, M., Zhao, W., Nyquist, P.A., Chen, C., Launer, L.J., Psaty, B.M., Ikram, M.K., Vernooij, M.W., Schmidt, H., Pausova, Z., Becker, D.M., De Jager, P.L., Thompson, P.M., van Duijn, C.M., Bennett, D.A., Slagboom, P.E., Schmidt, R., Longstreth, W.T., Ikram, M.A., Seshadri, S., Debette, S., Gudnason, V., Adams, H.H.H., DeCarli, C., 2019. A genome-wide association study identifies genetic loci associated with specific lobar brain volumes. Commun. Biol. 2, 285.

Madan, C.R., 2018. Age differences in head motion and estimates of cortical morphology. PeerJ 6, e5176.

Madan, C.R., Kensinger, E.A., 2017. Test-retest reliability of brain morphology estimates. Brain Inf. 4, 107–121.

Madre, M., Canales-Rodriguez, E.J., Fuentes-Claramonte, P., Alonso-Lana, S., Salgado-Pineda, P., Guerrero-Pedraza, A., Moro, N., Bosque, C., Gomar, J.J., Ortiz-Gil, J., Goikolea, J.M., Bonnin, C.M., Vieta, E., Sarro, S., Maristany, T., McKenna, P.J., Salvador, R., Pomarol-Clotet, E., 2019. Structural abnormality in schizophrenia versus bipolar disorder: a whole brain cortical thickness, surface area, volume and gyrification analyses. Neuroimage Clin. 25, 102131.

Marcus, D.S., Olsen, T.R., Ramaratnam, M., Buckner, R.L., 2007. The extensible neuroimaging archive toolkit: an informatics platform for managing, exploring, and sharing neuroimaging data. Neuroinformatics 5, 11–34.

Matsuda, Y., Ohi, K., 2018. Cortical gyrification in schizophrenia: current perspectives. Neuropsychiatric Dis. Treat. 14, 1861–1869.

Mende, M.A., 2019. Alcohol in the aging brain - the interplay between alcohol consumption, cognitive decline and the cardiovascular system. Front. Neurosci. 13, 713.

Nesvag, R., Schaer, M., Haukvik, U.K., Westlye, L.T., Rimol, L.M., Lange, E.H., Hartberg, C.B., Ottet, M.C., Melle, I., Andreassen, O.A., Jonsson, E.G., Agartz, I., Eliez, S., 2014. Reduced brain cortical folding in schizophrenia revealed in two independent samples. Schizophr. Res. 152, 333–338.

Ossenkoppele, R., Smith, R., Ohlsson, T., Strandberg, O., Mattsson, N., Insel, P.S., Palmqvist, S., Hansson, O., 2019. Associations between tau, abeta, and cortical thickness with cognition in alzheimer disease. Neurology 92, e601–e612.

Palaniyappan, L., Liddle, P.F., 2012. Aberrant cortical gyrification in schizophrenia: a surface-based morphometry study. J. Psychiatry Neurosci. 37, 399–406.

Pfefferbaum, A., Sullivan, E.V., 2015. Cross-sectional versus longitudinal estimates of age-related changes in the adult brain: overlaps and discrepancies. Neurobiol. Aging 36, 2563–2567.

Price, C.J., 2012. A review and synthesis of the first 20 years of pet and fmri studies of heard speech, spoken language and reading. Neuroimage 62, 816–847.

R Core Team R, 2016. A Language and Environment for Statistical Computing. R Foundation for Statistical Computing, Vienna, Austria.

Richman, D.P., Stewart, R.M., Hutchinson, J.W., Caviness Jr., V.S., 1975. Mechanical model of brain convolutional development. Science 189, 18–21.

Rubin, D.B., 1987. Multiple Imputation for Nonresponse in Surveys. John Wiley & Sons, New York.

Schaer, M., Cuadra, M.B., Tamarit, L., Lazeyras, F., Eliez, S., Thiran, J.P., 2008. A surface-based approach to quantify local cortical gyrification. IEEE Trans. Med. Imag. 27, 161–170.

Schaer, M., Cuadra, M.B., Schmansky, N., Fischl, B., Thiran, J.P., Eliez, S., 2012. How to measure cortical folding from mr images: a step-by-step tutorial to compute local gyrification index. JoVE e3417.

Schippling, S., Ostwaldt, A.C., Suppa, P., Spies, L., Manogaran, P., Gocke, C., Huppertz, H.J., Opfer, R., 2017. Global and regional annual brain volume loss rates in physiological aging. J. Neurol. 264, 520–528.

Taki, Y., Thyreau, B., Kinomura, S., Sato, K., Goto, R., Kawashima, R., Fukuda, H., 2011. Correlations among brain gray matter volumes, age, gender, and hemisphere in healthy individuals. PloS One 6, e22734.

Tan, P.K., Ananyev, E., Hsieh, P.J., 2019. Distinct genetic signatures of cortical and subcortical regions associated with human memory. eNeuro 6.

Taylor, P., Hobbs, J.N., Burroni, J., Siegelmann, H.T., 2015. The global landscape of cognition: hierarchical aggregation as an organizational principle of human cortical networks and functions. Sci. Rep. 5, 18112.

Tiffin, J., Asher, E.J., 1948. The purdue pegboard; norms and studies of reliability and validity. J. Appl. Psychol. 32, 234–247.

Vinke, E.J., de Groot, M., Venkatraghavan, V., Klein, S., Niessen, W.J., Ikram, M.A., Vernooij, M.W., 2018. Trajectories of imaging markers in brain aging: the rotterdam study. Neurobiol. Aging 71, 32–40.

Vliegenthart, R., Geleijnse, J.M., Hofman, A., Meijer, W.T., van Rooij, F.J., Grobbee, D.E., Witteman, J.C., 2002. Alcohol consumption and risk of peripheral arterial disease: the rotterdam study. Am. J. Epidemiol. 155, 332–338.

Welsh, K.A., Butters, N., Mohs, R.C., Beekly, D., Edland, S., Fillenbaum, G., Heyman, A., 1994. The consortium to establish a registry for alzheimer's disease (cerad). Part v. A normative study of the neuropsychological battery. Neurology 44, 609–614.

White, T., Su, S., Schmidt, M., Kao, C.Y., Sapiro, G., 2010. The development of gyrification in childhood and adolescence. Brain Cognit. 72, 36–45.

White, T., Jansen, P.R., Muetzel, R.L., Sudre, G., El Marroun, H., Tiemeier, H., Qiu, A., Shaw, P., Michael, A.M., Verhulst, F.C., 2018. Automated quality assessment of structural magnetic resonance images in children: comparison with visual inspection and surface-based reconstruction. Hum. Brain Mapp. 39, 1218–1231.

Wood, R.L., 2017. Accelerated cognitive aging following severe traumatic brain injury: a review. Brain Inj. 31, 1270–1278.

Xu, G., Knutsen, A.K., Dikranian, K., Kroenke, C.D., Bayly, P.V., Taber, L.A., 2010. Axons pull on the brain, but tension does not drive cortical folding. J. Biomech. Eng. 132, 071013.

Yang, H., Xu, H., Li, Q., Jin, Y., Jiang, W., Wang, J., Wu, Y., Li, W., Yang, C., Li, X., Xiao, S., Shi, F., Wang, T., 2019. Study of brain morphology change in alzheimer's disease and amnestic mild cognitive impairment compared with normal controls. Gen. Psychiatr. 32, e100005.

Zilles, K., Palomero-Gallagher, N., Amunts, K., 2013. Development of cortical folding during evolution and ontogeny. Trends Neurosci. 36, 275–284.